Interference photoconductivity and photoelectromagnetic effect in amorphous silicon

Vincenzo Augelli and Roberto Murri
Dipartimento di Fisica, Università degli Studi di Bari, via Amendola 173, I-70126 Bari, Italy

Marian Nowak
Institute of Physics, Silesian Technical University, PL-44-100 Gliwice, Poland
(Received 8 July 1988)

The existence of the so-called interference photoconductivity (PC) and photoelectromagnetic (PEM) effects in the investigated thin films of *a*-Si:H,F is shown. These effects appear due to interference of radiation in a sample. In this paper, the fitting of interference PC and PEM responses to theoretical relationships is presented. Values of carrier lifetime, diffusion length, and surface recombination velocity have been estimated. Spectral dependences of individual quantum efficiency coefficients for PC and PEM effects can give information about energy distribution and type of electronic states in the investigated samples. Influence of radiation intensity on optical and recombination parameters of the material is shown.

I. INTRODUCTION

One of the purposes of investigations on photoconductivity (PC) and photoelectromagnetic (PEM) effect is to determine the values of semiconductor parameters. In fact, both effects are dependent on (see, e.g., Refs. 1 and 2) carried lifetimes (τ_e,τ_h), recombination velocities of electrons and holes at the front (illuminated) (s_1,s_{1h}) and back (s_2,s_{2h}) sample surfaces, drift and Hall mobilities of electrons and holes ($\mu_e,\mu_h,\mu_{He},\mu_{Hh}$), electron and hole concentrations (n_e,n_h), quantum efficiency coefficient of the incident radiation (β), and complex refractive index of the semiconductor ($n-i\kappa$). In the case of extrinsic semiconductors, PC measurements yield information about the majority carriers because of trapping of the minority carriers (semi-insulating GaAs may be a rare exception). PEM effect is connected with a diffusion process, so it is controlled by the transport and recombination parameters of the minority carriers. Additionally, the quantum efficiency coefficient has different spectral dependences for PC and PEM effect. Contrary to PC, the PEM effect occurs essentially in the case of interband (intrinsic) photoexcitation of electrons and holes. The so-called impurity PEM effect can be observed only in the case of extrinsic photogeneration of minority carriers (see, e.g., Refs. 3 and 4). Therefore, PC and PEM effect have attracted considerable interest as a potential tool in investigations of many problems related to the fundamental properties of semiconductors.[2] They have been studied not only in many crystalline semiconductor materials but also in amorphous silicon. The first observation of PEM effect in *a*-Si:H, and the use of it for estimation of carrier mobility and lifetime, was reported by Moore.[5]

In this paper we shall show the influence of the interference of the radiation internally reflected in a thin sample of *a*-Si:H,F on the PC and PEM responses. The additional contributions to the PEM effect and PC due to the interference effect are known as interference PEM effect and interference PC (see, e.g., Refs. 2, 6, and 7 and references therein). Oscillatory dependences of these contributions on photon energy, sample thickness, and angle of incidence of radiation are the most characteristic features for them. Actually, such dependences are mainly due to the influence of semiconductor thickness, wavelength, and angle of incidence of radiation on the effective light intensity entering a thin, parallel-sided semiconductor film similar to a Fabry-Pérot resonator. This influence is of the same nature as that one which determines the interference fringes in optical reflectivity from the sample. However, the spatial distribution of excess carriers, i.e., intensity of radiation which generates the carriers, over sample thickness is also important for the PC and especially for PEM effect. In the case of interference, this spatial distribution has the characteristic form of stationary wave light which is well known since Wiener's experiments.[8] This specific spatial distribution of carriers can also affect the interference PC and PEM effect.

II. EXPERIMENTAL RESULTS

All measurements were performed at room temperature on thin films of *a*-Si:H,F deposited on Corning Glass 7059 substrates. They were prepared using a capacitively coupled glow-discharge system with SiF_4-H_2 mixture. The mixture composition $[H_2]/[SiF_4]$ was 0.1. The discharge pressure was 0.3 Torr, rf power was estimated at 13 W, and the deposition temperature was 300 °C. Deposition details are reported elsewhere.[9] For PC and PEM measurements the specimens were equipped with two Al evaporated contacts in coplanar configuration and 1.5 mm apart. The length of the illuminated area was 3.5 mm.

The optical transmission (T) spectra for samples were measured with a Cary 118CX spectrophotometer in the wavelength range from 540 to 900 nm. A typical set of experimental results for a sample 0.76 μm thick is presented in Fig. 1. The characteristic interference fringes are seen for low photon energies.

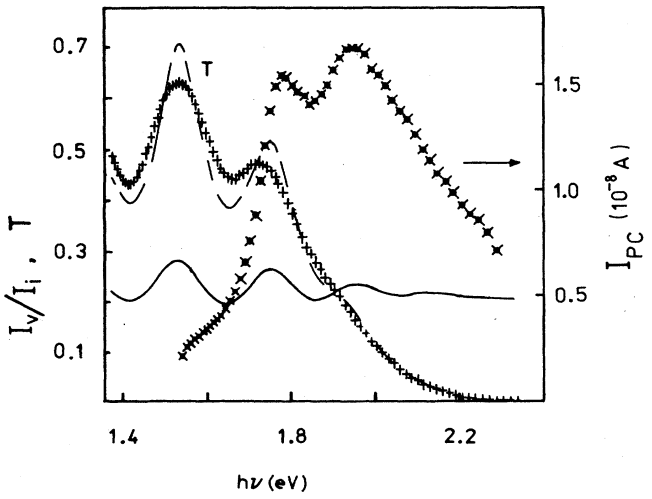

FIG. 1. Optical transmittance (+) and PC current (×) of a 0.76-μm-thick film of a-Si:H,F vs photon energy (PC responses measured for $I_i = 10^{18}$ photons/m^2 s). Dashed curve represents theoretical transmittance calculated for $\delta = 1$, and the n and k values shown in Figs. 9 and 10. Spectral dependence of the transmittance calculated for $\delta = 0.6$ cannot be practically distinguished from experimental data (+). Solid curves represents the effective intensity of radiation which enters the semiconductor ($\delta = 0.6$).

The photocurrent I_{PC} was measured using a Keithley 619 electrometer controlled by a Hewlett-Packard-HP85 computer. The bias voltage was taken from a 6516A dc Hewlett-Packard power supply. The photocurrent-voltage characteristic was linear in a relatively medium range (Fig. 2). Spectral investigations of PC and PEM effects were performed using a high-intensity Bausch-Lomb monochromator. The photon flux I_i incident on the sample was measured by means of a pyroelectric radiation detector Molectron P4-450. Some experimental results were obtained using a He-Ne Hughes laser 3225 H-C. The light intensity was changed in the four-decade range using neutral filters. The existence of some extrema and inflection points was typical for spectral characteristics of PC (Figs. 1 and 3). One can note that the ratio of the photocurrent to the illumination intensity decreases with the increase of intensity (Fig. 3). But the radiation intensity not only influences the magnitude of the photocurrent, it also changes qualitatively the shape of its spectral characteristics (compare the data in Figs. 1 and 3). The decrease of the photocurrent with increasing absorption coefficient, k, is greater for higher light intensity. The relationship between photocurrent and light intensity was well fitted in a wide range of I_i by

$$I_{PC} = a_1 I_i^{\alpha_{PC}} \tag{1}$$

power law (Fig. 4) with a_1 and α_{PC} parameters dependent on wavelength of radiation (see Figs. 4 and 5). In the wavelength range from 540 to 720 nm the power coefficient α_{PC} was well fitted by the linear formula

$$\alpha_{PC} = a_2 h\nu + a_3 \tag{2}$$

in which $a_2 = -0.263 \pm 0.008$ eV^{-1} and $a_3 = 1.31 \pm 0.02$. Unfortunately, explanation of this empirical formula is very difficult because PC current is a very complicated function of many parameters which can be dependent on wavelength and intensity of radiation [see Eq. (22)].

PEM measurements were performed with the magnetic-field single modulation technique at 20 Hz. An electromagnet was supplied by a Wavetek 186 generator through a 500-W power amplifier. ac PEM short-circuit current (I_{PEM}) was measured by using a two-phase lock-in analyzer (5206 Brookdeal Electronics) with 5002 current preamplifier controlled also by a Hewlett-Packard 85 computer. Open-circuit PEM voltages were also measured, but because the theoretical analysis is much more cumbersome[2] without giving any new infor-

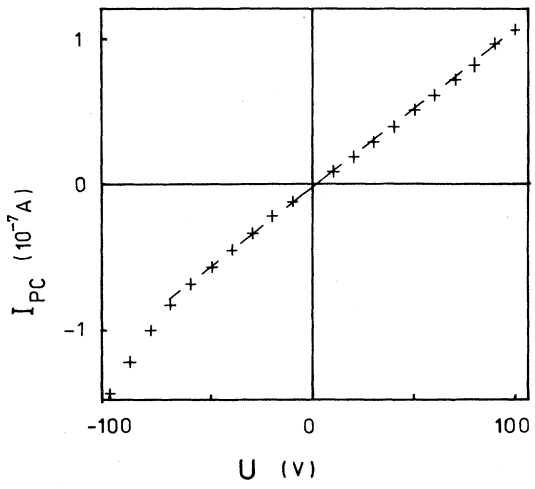

FIG. 2. PC current vs electric field ($\lambda = 0.6328$ μm). Dashed curve represents the linear dependence.

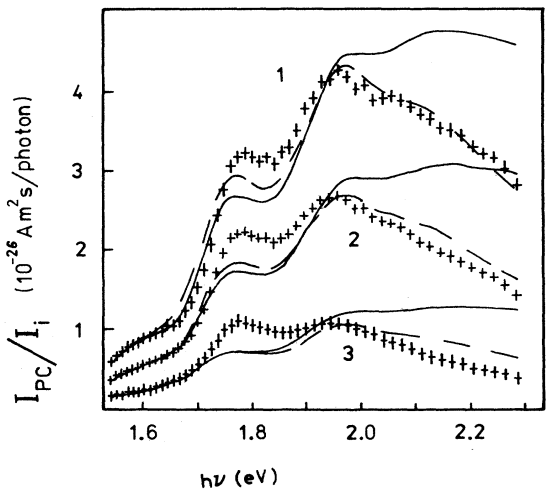

FIG. 3. Normalized PC currents in a 0.76-μm-thick film of a-Si:H,F vs photon energy for different intensities of radiation (1:10^{16}, 2:10^{17}, 3:10^{19} photons/m^2 s). Solid and dashed curves represent the best fitting for conditions $W \gg 1$ and $W \ll 1$, respectively.

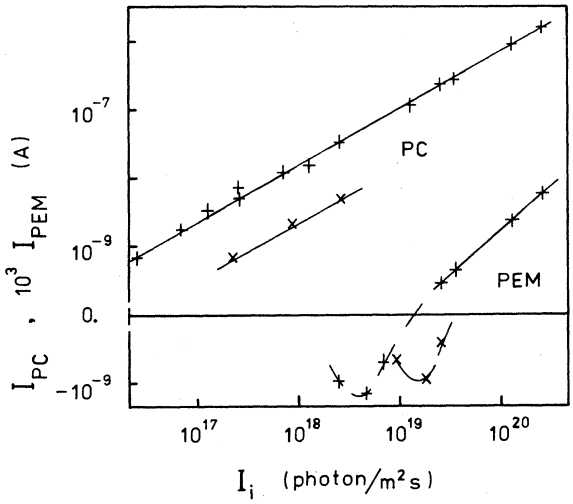

FIG. 4. PC and PEM currents vs radiation intensity for 0.633 μm (+) and 0.800 μm (×) wavelength of radiation. Solid curves represent the power law of the form (1).

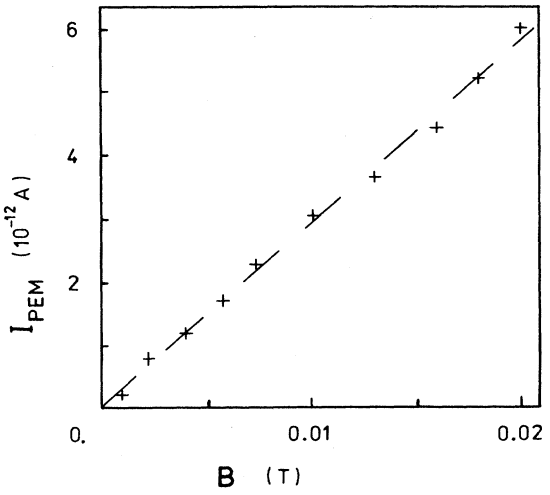

FIG. 6. PEM current vs magnetic field (λ=0.6328 μm). Dashed curve represents the linear dependence.

mation, they are not presented in this paper.

We observed linear dependence of I_{PEM} on magnetic field (Fig. 6) (typical for semiconductors with low mobility carriers). PEM photoresponse was a more cumbersome function of photon energies (Fig. 7) and light intensity (Fig. 4) than PC photoresponse. For smaller radiation intensities the so-called negative PEM effect was observed. This effect occurs under certain experimental conditions, e.g., if due to a fast recombination of carriers at the front of an optically thin sample ($K=wk=4\pi\kappa w/\lambda \leq 1$), some carriers flow towards the illuminated surface and this component of current flow exceeds that away from the surface due to diffusion and recombination at the back surface. So, in the negative PEM effect the sign of I_{PEM} is reversed to that which characterizes the PEM current in the case of very strong absorption of radiation in the investigated semiconductor. The observed negative PEM effect changed into the normal one with increasing radiation intensity (Fig. 4). The relationship between PEM current and illumination intensity could be described by a power law similar to Eq. (1) only for a narrow range of high radiation intensities (see the solid curve in Fig. 4). For radiation of wavelength λ=0.6328 μm and intensity in the range $(2-20)\times 10^{19}$ photons/m²s, the power coefficients in PC and PEM current-illumination power laws were equal to

$$\alpha_{PC}=0.82\pm0.01, \quad \alpha_{PEM}=1.31\pm0.01 . \tag{3}$$

However, for smaller radiation intensities, the power

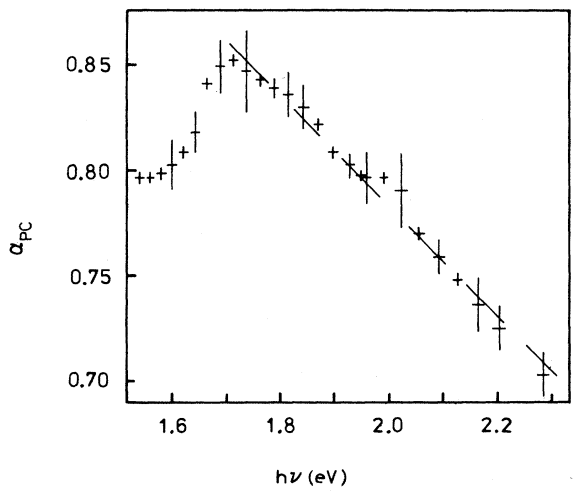

FIG. 5. Power coefficient from the power-law dependence of PC current on radiation intensity vs photon energy. Dashed curve represents the linear dependence (2).

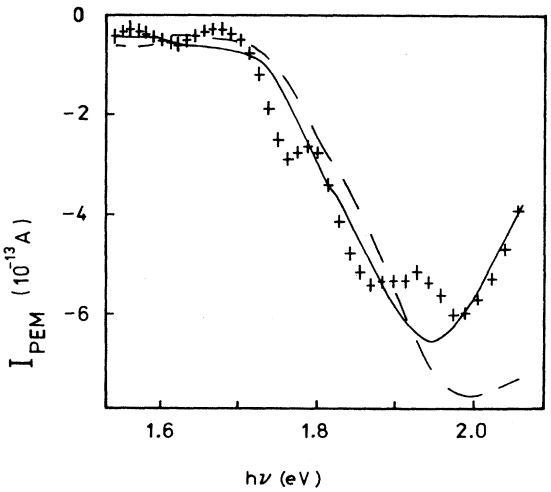

FIG. 7. PEM current vs photon energy ($I_i=10^{18}$ photons/m²s). Solid and dashed curves represent the best fitting for $W \gg 1$ and $W \ll 1$, respectively.

coefficient α_{PEM} was dependent not only on photon energy as α_{PC}, but was also strongly dependent on radiation intensity (see Fig. 8).

III. RESULTS AND DISCUSSION

A. Optical transmittance and spatial distribution of radiation intensity in a semiconductor

From an optical point of view, the investigated sample consists of a single, parallel-sided, homogeneous, and isotropic absorbing film of thickness w and complex refractive index $n-i\kappa$ on a nonabsorbing, parallel-sided substrate of thickness w_2 and refractive index n_2. This structure is bounded by a nonabsorbing medium of refractive index n_0. Radiation of wavelength λ hits perpendicularly the structure from the absorbing film side. Due to finite spectral bandwidth and relatively great thickness of the substrate ($\Delta\lambda \gg \lambda^2/2n_2w_2$) the effects of interference vanish in the substrate.

Since a single film bounded by two surfaces possesses an effective reflection coefficient and accompanying phase change, such a film may be replaced by a single surface having these properties. Such a procedure of simplifying a system of multiple films is usually used for determining reflectance and transmittance of films systems.[10] Therefore, to determine the optical transmittance of the substrate covered with the semiconductor films, we can simply calculate

$$T=\frac{T_1T_2}{1-R_1R_2}\ , \tag{4}$$

where T_1 and R_1 represent the effective transmittance and reflection coefficient of the semiconductor film which covers the front surface of the substrate, and T_2 and R_2 describe transmittance and reflectance from the back surface of the substrate:

$$T_2=\frac{4n_2^2}{(n_2+n_0)^2},\quad R_2=\frac{(n_0-n_2)^2}{(n_0+n_2)^2}\ . \tag{5}$$

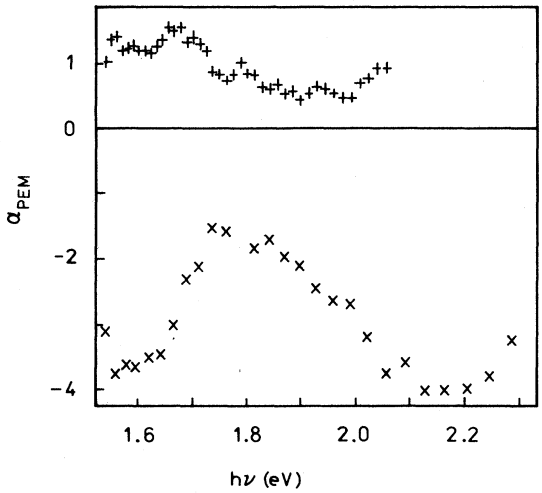

FIG. 8. Power coefficient from the power-law dependence of PEM current on radiation intensity vs photon energy (+, $I_i=2\times10^{18}$; ×, $I_i=7\times10^{18}$ photons/m^2 s).

Using the well-known formulas for the effective transmittance and reflection coefficient of the semiconductor film (a simple interference filter) the following relationship can be obtained:

$$T=I_v t_2^2 T_2 e^{-K}\ , \tag{6}$$

where I_v represents the effective intensity of radiation which enters the semiconductor and is given by

$$I_v=\frac{t_1^2}{1-r_2^2R_2+r_1^2e^{-2K}[(2\delta-1)r_2^2-R_2]+2\delta r_1r_2e^{-K}[\cos(\psi+\varphi-\Gamma)-R_2\cos(\psi-\varphi+\Gamma)]}\ , \tag{7}$$

where

$$\Gamma=4\pi nw/\lambda,\quad K=wk=4\pi\kappa w/\lambda\ ,$$

$$t_1^2=\frac{4n_0^2}{(n+n_0)^2+\kappa^2},\quad r_1^2=\frac{(n-n_0)^2+\kappa^2}{(n+n_0)^2+\kappa^2}\ ,$$

$$t_2^2=\frac{4(n^2+\kappa^2)}{(n+n_2)^2+\kappa^2},\quad r_2^2=\frac{(n-n_2)^2+\kappa^2}{(n+n_2)^2+\kappa^2}\ ,$$

$$\sin\varphi=\frac{2n_0\kappa}{[(n+n_0)^2+\kappa^2]r_1}\ , \tag{8}$$

$$\cos\varphi=\frac{n_0^2-n^2-\kappa^2}{[(n+n_0)^2+\kappa^2]r_1}\ ,$$

$$\sin\psi=\frac{-2n_2\kappa}{[(n+n_2)^2+\kappa^2]r_2}\ ,$$

$$\cos\psi=\frac{n^2+\kappa^2-n_2^2}{[(n+n_2)^2+\kappa^2]r_2}\ .$$

Parameter δ represents the so-called coherence factor. It is a semiempirical coefficient which was introduced into the mathematically derived formulas to improve agreement between theory and experimental results. When the coherence of radiation beams, internally reflected in the semiconductor film, is negligible, e.g., in the presence of wave-front deformations in an inhomogenous film or in a sample with nonparallel or rough surfaces, $\delta=0$ and Eq. (6) is identical to the well-known formula describing transmittance of radiation in the absence of interference effects. For $\delta=1$, Eq. (6) describes the case of fine interference in the optical filter.

Using the experimental dependence of optical transmittance on photon energy (Fig. 1), the values of n were estimated from the extrema conditions at the interference fringes, as it was done, e.g., in Ref. 10. Then the obtained values were approximated assuming the single oscillator dispersion law[11]

$$n^2=1+\frac{A_1}{E_1^2-(h\nu)^2} \tag{9}$$

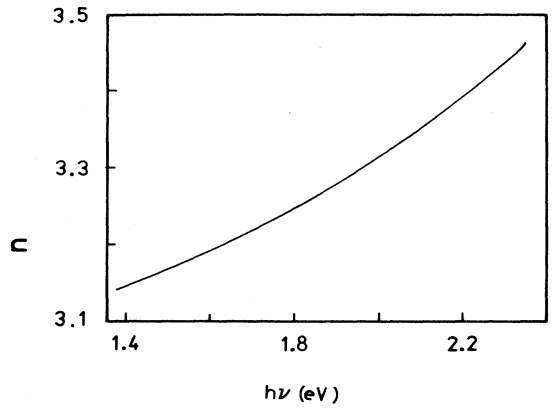

FIG. 9. Real part of refractive index of 0.76-μm-thick film of a-Si:H,F.

in which the values of average band gap $E_1=4.56$ eV, and the coefficient $A_1=167$ (eV)^2, proportional to electron density were found. Taking such approximated values of n (presented in Fig. 9), and assuming different values of coherence factor δ, the values of absorption coefficient k were determined fitting numerically formula (6) with the experimental data. The best fitting was achieved for $\delta=0.6$. Spectral dependence of the fitted values of absorption coefficient k is represented by curve 4 in Fig. 10. Spectral dependence of transmittance calculated for these values of k, the values of n shown in Fig. 9, and $\delta=0.6$ cannot be practically distinguished from the experimental data shown in Fig. 1. The dashed curve in Fig. 1 represents only the values of T calculated for the same values of k and n but for the fine interference ($\delta=1$). It can be concluded from the best-fitted value of $\delta=0.6$ that the investigated a-Si film was slightly inhomogeneous, and this disturbs the interference phenomenon in it.

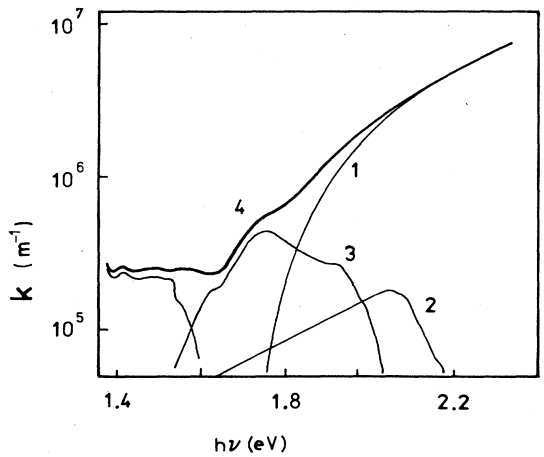

FIG. 10. Spectral dependence of absorption coefficient of radiation of 0.76-μm-thick film of a-Si:H,F [1, k_f estimated from Eq. (10); 2, k_u estimated for Urbach rule (19); 3, k_{ex} estimated for intrinsic photogeneration of carriers; 4, total absorption coefficient k estimated from the optical transmittance of the film].

If one uses the conventional dispersion formula describing absorption coefficient k_f characteristic for photogeneration of carriers from the top of extended states in the valence band to the extended states in the conduction band, namely

$$k_f h\nu = A_2(h\nu - E_0)^2 \tag{10}$$

for fitting the values of k (estimated for higher photon energies), the values of optical gap $E_0=1.72\pm0.01$ eV, and the constant $A_2=46$ m/eV (proportional to the joint density of states in the valence and conduction bands) can be found. The spectral dependence of approximated values of k_f is shown in Fig. 10 (curve 1).

Using the same procedure as for optical transmittance, and as was done, e.g., in Ref. 6, it is relatively easy to obtain the following formula for the distribution of radiation intensity through semiconductor thickness:

$$I=I_v[g_1e^{-ky}+g_2e^{ky-2K}+g_3e^{-K}\cos(\gamma y-\psi+\Gamma)] , \tag{11}$$

where

$$g_1=1+\frac{r_2^2+R_2}{1-r_2^2R_2}r_1^2e^{-K} ,$$
$$g_2=r_2^2+\frac{r_2^2+R_2}{1-r_2^2R_2} , \tag{12}$$
$$g_3=2r_2, \quad \gamma=4\pi n/\lambda ,$$

y represents the depth in the semiconductor film, and the other parameters are the same as in Eq. (6).

In the case of strong absorption, I decreases exponentially with increasing distance traveled in the sample. In the case of optically thin sample ($K<1$), a stationary light wave occurs in the semiconductor due to the interference of radiation internally reflected from its surfaces [the third component in Eq. (11)], as was first observed in the well-known experiments by Wiener.[8]

The solid curve in Fig. 1 shows the spectral dependence of I_v calculated for $\delta=0.6$, and n and k taken from Figs. 9 and 10. This effective intensity of radiation which enters the 0.76-μm-thick film of a-Si:H,F corresponds with the optical transmittance of the film. However, one can see that the interference fringes occur in the $I_v(h\nu)$ curve in the wavelength range in which the transmittance is practically a monotonous function of photon energy. Hence, in this spectral range, the interference fringes must be more evident in spectral characteristics of photoelectric effects, e.g., PC and PEM, than in optical transmittance (see, e.g., Fig. 1), as long as the photoelectric responses are proportional to I_v.

B. Photoelectromagnetic effect

In the present case, the conditions under which the PEM effect occur are as follows: (a) an isotropic, uniform throughout its volume, parallel-sided semiconductor film

of thickness w and refractive index $n-i\kappa$ is placed in a homogeneous magnetic field $\mathbf{B}(0,0,B)$; (b) the film is infinite in the XZ plane and it covers a nonabsorbing substrate of refractive index n_2 and thickness w_2; (c) the sample is bounded in the Y direction by a nonabsorbing medium of refractive index n_0; (d) radiation of wavelength λ propagates in the Y direction and its intensity in the semiconductor film is described by Eq. (11); (e) semiconductor parameters have their values appropriate for the used conditions; (f) the effect of a surface space-charge layer can be ignored; (g) in the considered steady state $G_e-R_e=G_h-R_h$ (where G_e,G_h,R_e,R_h represent the photogeneration and recombination rates for electrons and holes, respectively).

If we assume additionally that the concentration of optically excited carriers remains much less than that of carriers normally present in the unilluminated sample ($\Delta n_e \ll n_e$, $\Delta n_h \ll n_h$), the expression of the short-circuit PEM current can be relatively easily found (see the Appendix):

$$
\begin{aligned}
i_{\mathrm{PEM}} &= (\mu_{He}+\mu_{Hh})Bewl_z\beta_{\mathrm{PEM}}I_v \\
&\times \left[\frac{g_1 K}{(K^2-W^2)R}\{[W+S_2+(W-S_2)e^{-2W}-2We^{-W}](K+S_1) \right. \\
&\qquad +[W+S_1+(W-S_1)e^{-2W}-2We^{-W}](K-S_2)e^{-K}-(1-e^{-K})R\} \\
&\quad -\frac{g_2 K e^{-K}}{(K^2-W^2)R}(\{(K+S_2)[W+S_1-(W-S_1)e^{-W}] \\
&\qquad +(K-S_1)[W+S_2-(W-S_2)e^{-W}]e^{-K}\}(1-e^{W})-(1-e^{-K})R) \\
&\quad -\frac{2g_3 K e^{-K}}{R(W^2+\Gamma^2)}((1-e^{-W})\{(\Gamma\sin\psi-S_2\cos\psi)[W+S_1-(W-S_1)e^{-W}] \\
&\qquad +[\Gamma\sin(\psi-\Gamma)+S_1\cos(\psi-\Gamma)][W+S_2-(W-S_2)e^{-W}]\} \\
&\qquad \left. +R[\cos\psi-\cos(\psi-\Gamma)]) \right]
\end{aligned}
\tag{13}
$$

for $kL\neq 1$,

$$
\begin{aligned}
&W=w/L, \quad L^2=D\tau_{\mathrm{PEM}}, \\
&S_1=s_1\tau_e w/L^2, \quad S_2=s_2\tau_e w/L^2, \\
&R=(W+S_1)(W+S_2)-(W-S_1)(W-S_2)e^{-2W}, \qquad (14) \\
&\tau_{\mathrm{PEM}}=\frac{n_e\tau_h+n_h\tau_e}{n_e+n_h}, \\
&D=\frac{(n_e+n_h)D_eD_h}{(1+\mu_{Hh}^2B^2)D_en_e+(1+\mu_{He}^2B^2)D_hn_h}.
\end{aligned}
$$

The coefficient τ_{PEM} represents the effective carrier lifetime deduced from PEM investigations (usually the minority carrier lifetime). The β_{PEM} represents the effective quantum efficiency coefficient for the PEM effect (usually the quantum efficiency coefficient for photogeneration of minority carriers):

$$
\beta_{\mathrm{PEM}}=\frac{n_h\tau_e\beta_e+n_e\tau_h\beta_h}{n_h\tau_e+n_e\tau_h}, \tag{15}
$$

where

$$
\beta_e=\frac{k_e}{k}\eta, \quad \beta_h=\frac{k_h}{k}\eta, \tag{16}
$$

η represents the number of carriers generated by one photon (in the following we assume that $\eta=1$), k represents the total absorption coefficient which affects the spatial distribution of radiation in a sample, and k_e and k_h represent absorption coefficient describing absorption processes in which the free electrons and holes are photogenerated, respectively. Parameter l_z represents the width of the sample. The other parameters have the same meanings as for Eq. (6).

The expression obtained from Eq. (13) for intrinsic photogeneration of carriers ($\beta_e=\beta_h$) is identical to that derived, e.g., in Refs. 2 and 6 under assumption of normal incidence of light into a sample. It must be underlined that for $r_2=R_2=0$, $t_1=1$, $\beta_e=\beta_h$, and $(\mu_{He}+\mu_{Hh})B \ll 1$, Eq. (13) is identical to the formula derived by Schetzina[12] for PEM current in relaxation semiconductors. In such materials, e.g., in high resistivity crystalline or amorphous semiconductors, the dielectric relaxation time is much greater than carrier lifetimes and the bulk charge neutrality is controlled overall by rapid recombination, whereas, in the so-called lifetime semiconductors (with carrier lifetime greater than dielectric relaxation time), the charge neutrality is maintained at equilibrium through fast dielectric relaxation processes. The formal identity of the descriptions of PEM effect in lifetime and relaxation semiconductors was first noticed by Look.[4]

Unfortunately, analytical formulas describing PEM effect for higher radiation intensities in a thin semiconductor film were not published up to now. So, Eq. (13) must be used in this paper as a first theoretical approximation of the observed PEM results. Of course, in this case, each of the semiconductor parameters involved in Eq. (13) has so-called high photoexcitation value, which

can depend on light intensity and can be different from the appropriate value for small illumination conditions. It must be noted, however, that Eq. (A5) is still valid for the large signal case ($\Delta n_e \gg n_e$, $\Delta n_h \gg n_h$) with the additional restrictions $\beta_e kI \gg \mathrm{div}\mathbf{I}_e/e$, $\beta_h kI \gg \mathrm{div}\mathbf{I}_h/e$. In such a case, n and p in Eqs. (14) and (15) must be replaced by Δn and Δp, respectively. Therefore, our analysis cannot describe PEM effect in the intermedium injection range ($\Delta n_e \simeq n_e$, $\Delta n_h \simeq n_h$). A similar method of analysis of PEM responses under strong illumination was used, e.g., in Ref. 13.

Assuming for the first step approximation $\beta_{\mathrm{PEM}}=1$, and taking the appropriate values of I_v, g_1, g_2, g_3 (calculated for $\delta=0.6$ and the values of n and k shown in Figs. 9 and 10), the experimental data were fitted using Eq. (13) with the numerical fitting method quoted in Chap. 6.2.4 and Ref. 2. Then we calculated the normalized ratio of the theoretically calculated i_{PEM} to the measured I_{PEM} current

$$\beta^*(h\nu)=\frac{i_{\mathrm{PEM}}}{I_{\mathrm{PEM}}\beta^*_{\max}} , \tag{17}$$

where $\beta^*_{\max}$ represents the maximum value of $\beta^*(h\nu)$, i.e., $\beta^*_{\max}=(i_{\mathrm{PEM}}/I_{\mathrm{PEM}})_{\max}$.

Such normalization is the consequence of the assumption that for photons of high energy, β_{PEM} saturates with the value $\beta_{\mathrm{PEM}}=1$. Comparing Fig. 7 with Figs. 10 and 11 one can note that the PEM responses were also measured for photon energies smaller than the optical gap E_0. Hence, excess carriers, the existence of which is necessary to the PEM phenomenon, are photogenerated not only due to the fundamental absorption described by k_f. To find the appropriate value of β_{PEM} we assumed that $k_e=k_h=k_f+k_u$, where k_u represents the absorption process which obeys the Urbach rule. Taking the calculated value of β^* as a second step approximation of β_{PEM}, the first approximation values k_u^* of the Urbach absorption coefficient were derived from the following formula:

$$k_u^*=\beta^* k-k_f . \tag{18}$$

Spectral characteristic of these values was fitted by the formula describing the Urbach rule

$$k_u=k_0\exp[(h\nu-E_2)/E_3] . \tag{19}$$

Curve 2 in Fig. 10 shows the values of such estimated coefficient k_u. From the approximation, the value $E_3=0.305$ eV of the width of the exponential tail in Urbach spectral dependence of absorption coefficient was found, as well as the value of $(\ln k_0-E_2/E_3)=(5.4\pm1.1)$.

Then we calculated the effective quantum coefficient

$$\beta_{\mathrm{PEM}}=\frac{k_f+k_u}{k}\eta , \tag{20}$$

the spectral characteristic of which is shown by curve 4 in Fig. 11.

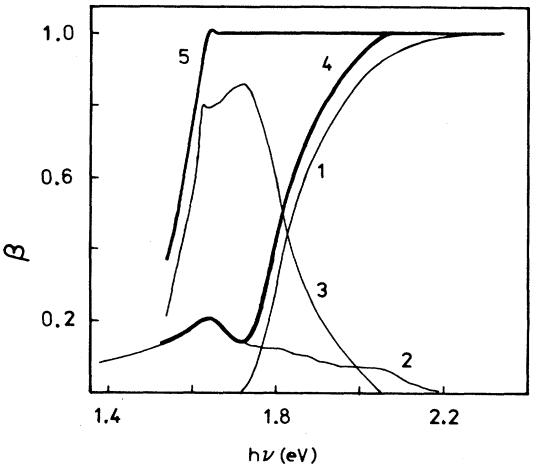

FIG. 11. Spectral dependence of quantum efficiency coefficients of radiation in 0.76-μm-thick film of a-Si:H,F (1, k_f/k; 2, k_u/k; 3, k_{ex}/k; 4, β_{PEM}; 5, β_{PC}).

Using the found values of β_{PEM}, and the appropriate values of I_v, g_1, g_2, g_3 (calculated for $\delta=0.6$ and the values of n and k shown in Figs. 9 and 10), we fitted the spectral dependence of I_{PEM}. The method quoted above of numerical fitting was used. From the fitted values of W, S_1, S_2 it was found that $S_1 \gg (W+S_2) \gg K$, $W \gg 1$, and $S_1 \gg \Gamma \gg 1$. Under this condition, Eq. (13) reduces to

$$i_{\mathrm{PEM}}=a_4\beta_{\mathrm{PEM}} I_v K e^{-K} , \tag{21}$$

where

$$a_4=-(\mu_{He}+\mu_{Hh})Bewl_z\frac{g_1+g_2}{W(W+S_2)} .$$

This best-fitting relationship is shown as a solid curve in Fig. 7. The general shape of this theoretical curve is in agreement with the spectral dependence of the measured short-circuit PEM current. The specific oscillatory discrepancies will be discussed in the conclusions. Unfortunately, the value of the parameter a_4 which was estimated during the fitting is a very cumbersome function of the microscopic transport and recombination parameters of the investigated semiconductor. So, in this case, it is not possible to obtain unique values of the semiconductor parameters (L, S_1, S_2). The estimated, rather important relations between the bulk and surface recombination parameters were already mentioned above.

C. Photoconductivity

If we take into consideration the same conditions as for the PEM effect but with electric field $\mathbf{E}(E,0,0)$ instead of the magnetic field, the photocurrent in the sample is described by (see the Appendix)

$$i_{PC}=(\mu_e+\mu_h)eEl_z\beta_{PEM}I_v\tau_{PC}$$
$$\times\left\{\frac{WK(1-e^{-W})}{(K^2-W^2)R}\{g_1[W_{s2}(K+S_1)-W_{s1}(K-S_2)e^{-K}]+g_2e^{-K}[(K+S_2)W_{s1}-(K-S_1)W_{s2}e^{-K}]\}\right.$$
$$-\frac{(1-e^{-K})K^2}{K^2-W^2}(g_1+g_2e^{-K})+\frac{2g_3Ke^{-K}}{R(W^2+\Gamma^2)}(W(1-e^{-W})\{(\Gamma\sin\psi-S_2\cos\psi)W_{s1}$$
$$-[\Gamma\sin(\psi-\Gamma)+S_1\cos(\psi-\Gamma)]W_{s2}\}$$
$$\left.-R\Gamma[\sin\psi-\sin(\psi-\Gamma)])\right|$$
$$+(\mu_e+\mu_h)eEl_z\beta_{PC}I_v\tau_{PC}\left[(1-e^{-K})(g_1+g_2e^{-K})+\frac{Kg_3e^{-K}}{\Gamma}[\sin\psi-\sin(\psi-\Gamma)]\right] \tag{22}$$

for $kL\neq 1$, where

$$\tau_{PC}=\frac{\tau_e\mu_e+\tau_h\mu_h}{\mu_e+\mu_h}, \tag{23}$$

$$\beta_{PC}=\frac{\mu_e\tau_e\beta_e+\mu_h\tau_h\beta_h}{\mu_e\tau_e+\mu_h\tau_h},$$

$$W_{s1}=W+S_1+(W-S_1)e^{-W}, \tag{24}$$

$$W_{s2}=W+S_2+(W-S_2)e^{-W}.$$

The effective quantum efficiency coefficient β_{PC} is typical for this component of PC response which is not dependent on the diffusion of the excess carriers [see the second term in formula (22)]. The other parameters have the same meanings as in Eq. (13).

The expression obtained from Eq. (22) for intrinsic photogeneration of carriers ($\beta_e=\beta_h$) is identical to that derived, e.g., in Refs. 6 and 7 under the assumption of normal incidence of light onto a sample. For the same reasons as those for the PEM effect, Eq. (22) is used in this paper to obtain pieces of information from the performed PC measurements. Of course, the same restrictions are valid as for the adequate theory of PEM effect.

Using the following relations between semiconductor parameters: $S_1\gg(W+S_2)\gg K$, $W\gg 1$, and $S_1\gg\Gamma\gg 1$, which were estimated in the PEM investigations, Eq. (22) reduces into

$$i_{PC}=(\mu_e+\mu_h)eEl_z\beta_{PC}I_v\tau_{PC}(1-e^{-K})(g_1+g_2e^{-K}). \tag{25}$$

The method of PC data treatment was similar to that used for PEM investigations. Assuming for the first step approximation $\beta_{PC}=1$, and taking the appropriate values of I_v,g_1,g_2,g_3 (calculated for $\delta=0.6$ and the values of n and k shown in Figs. 9 and 10), the experimental PC data (measured for the radiation intensity $I_i=10^{16}$ photons/m^2 s) were fitted using Eq. (22). The method quoted above of numerical fitting was used. Then we calculated the normalized ratio of the theoretically calculated i_{PC} to the measured I_{PC} current

$$\beta^{**}(h\nu)=\frac{i_{PC}}{I_{PC}\beta^{**}_{max}}, \tag{26}$$

where β^{**}_{max} represents the maximum value of $\beta^{**}(h\nu)$, i.e., $\beta^{**}_{max}=(i_{PC}/I_{PC})_{max}$.

The calculated values of β^{**} can be taken into account as the values of β_{PC}. Their spectral dependence is represented by curve 5 in Fig. 11. Comparing this curve with curve 4 in the same figure one can recognize that the excess carriers, which evoke the PC effect, must be originated due to some photogeneration process additional to those described by k_f and k_u coefficients. So, we can assume that in the PC phenomenon we observe the following quantum efficiencies for photogenerations of electrons and holes:

$$\beta_e=\frac{k_f+k_u+k_{ea}}{k}\eta,\quad \beta_h=\frac{k_f+k_u+k_{ha}}{k}\eta, \tag{27}$$

where k_{ea} and k_{ha} represent absorption coefficients describing the additional absorption processes (e.g., impurity absorption) in which the unipolar excess carriers (electrons and holes, respectively) are photogenerated.

Consequently to the assumptions taken one can find

$$\beta_{PC}=\frac{\mu_e\tau_ek_{ea}/k+\mu_h\tau_hk_{ha}/k}{\mu_e\tau_e+\mu_h\tau_h}\eta+\beta_{PEM}=\beta_{PCe}+\beta_{PEM} \tag{28}$$

where β_{PCe} represents the effective quantum efficiency coefficient which is characteristic to the PC response evoked by extrinsic photogeneration of unipolar excess carriers in the case of negligible diffusion effect. The spectral dependence of the estimate values of β_{PCe} is shown by curve 3 in Fig. 11. If one takes into account that β_{PCe} corresponds to the photogeneration of majority carriers, it is possible to estimate values of absorption coefficient k_{ex} which characterize the process of radiation absorption in which the carriers are generated. The estimated spectral dependence of k_{ex} is shown by curve 3 in Fig. 10.

Using the found values of β_{PC} and the approximate values of I_v,g_1,g_2,g_3 (calculated for $\delta=0.6$, and the values of n and k shown in Figs. 9 and 10), we fitted with formula (25) the spectral dependences of I_{PC} currents measured for different intensities of radiation. The quoted numerical fitting method was used. The fitted values of $(\mu_e\tau_e+\mu_h\tau_h)$ are shown in Fig. 12 as a function of light intensity impinging on the sample. They can be well approximated by the following power-law relationship:

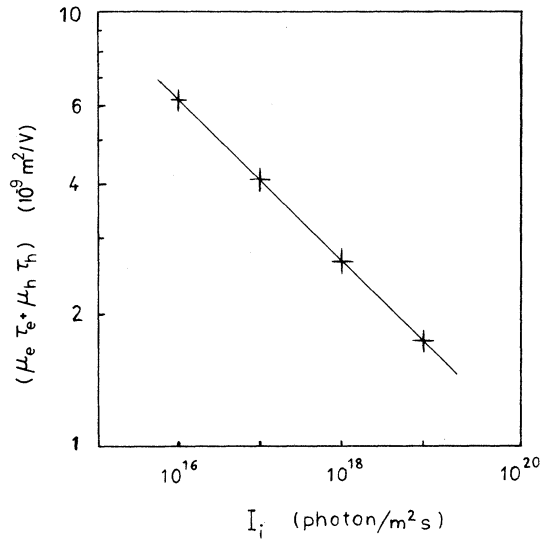

FIG. 12. Dependence of the products of carrier mobilities and lifetimes on light intensity incident on *a*-Si:H,F film [solid line represents the power-law relationship (29)].

$$(\mu_e \tau_e + \mu_h \tau_h) = a_6 I_i^{a_5} \tag{29}$$

in which $a_5 = -(0.191 \pm 0.001)$, $a_6 = (7.4 \pm 0.1) \times 10^{-6}$ m^2/V (when I_i is given in photons/m^2 s).

The decrease of the product of carrier lifetime and mobility with increasing intensity of radiation incident upon the *a*-Si:H,F film is evident in Fig. 3. The normalized PC response (or so-called PC response gain) strongly decreases with increasing light intensity. However, the essential problem is that the fitting of the experimental data with formula (25) is rather a poor one, especially for higher photon energies and radiation intensity (see the solid curves in Fig. 3). Let us analyze the case of smallest radiation intensity ($I_i = 10^{16}$ photons/m^2 s) which was used in our experiments. Up to 1.75 eV photon energy the fitted relationship (25) is very close to the experimental points. In the photon range 1.75–2.0 eV the theoretical curve describes well the general shape of the experimental spectral dependence of I_{PC}. It increases, attains maximum, slightly decreases, attains minimum, and then increases to the next maximum. The positions of the extrema of experimental and theoretical data coincide in the photon energy scale. Only the magnitudes of the first local maximum and minimum are too small in the fitted relation. For photon energies higher than 2.0 eV, the behavior of the theoretical curve is quite different from the spectral characteristic of measured PC current. The values of the measured I_{PC} rapidly decrease with increasing photon energy. With increasing light intensity the different behaviors of experimental and theoretically predicted PC responses start for smaller photon energies (compare cases 1 to 3 in Fig. 3). In the case of the highest light intensity ($I_i = 10^{19}$ photons/m^2 s) the local maximum of I_{PC} measured for smaller photon energy is higher than that for the higher photon energy. This is opposite the case of smaller radiation intensity, and to the behavior of the fitted theoretical relation. All the above-mentioned discrepancies between experiment and its theoretical description will be discussed in Sec. IV.

It must be noticed that one can make the fitting of the experimental data better, from a mathematical point of view, when one uses the general Eq. (22) without the restrictions on relations between semiconductor parameters (S_1, W, S_2) which were estimated in the PEM investigations. The dashed curves in Fig. 3 represent such fitted theoretical relations. In this case, from the fitted values of W, S_1, and S_2 it was found that $S_1 \gg 1 \gg W \gg S_2$ and $S_1 \gg \Gamma \gg 1$.

The result of the dimensionless front surface recombination velocity much greater than the bulk one and the back one is the same as obtained from PEM investigations. Unfortunately, the estimation of the sample thickness much less than the carrier diffusion length seems to be rather unrealistic. However, it is worth mentioning that even in the last case, with the assumption of $W \ll 1$ (when the PC theory predicts the decrease of PC current with increasing photon energy for relatively weakly absorbed radiation), the fitting is good only for small illumination of the sample. For large illumination it is still impossible to fit exactly the strong decrease of I_{PC} with increasing photon energy. The dashed curve in Fig. 7 represents the corresponding best fitting of the PEM results under the restriction of $W \ll 1$. This fitting is worse than that performed using Eq. (13) without any restrictions, and discussed formerly.

IV. CONCLUSIONS

Investigations of PC and PEM effects are a useful tool for determining the recombination, transport, and optical parameters of amorphous silicon. They should be efficiently applied to investigations of energetic spectrum of electronic states in this material, giving information about spectral dependences of individual quantum efficiency coefficients for photogeneration of minority and majority carriers.

Due to interference of radiation internally reflected in a thin film of amorphous silicon, the dependences of PC and PEM responses on photon energy and thickness of the film have an oscillatory character. In this case, the PC and PEM phenomena are known as the interference PC and interference PEM effects. It must be taken into serious consideration when values of semiconductor parameters are determined from the PC or PEM measurements.

In the investigated films of *a*-Si:H,F the recombination of excess carriers at the free surface prevails over the recombination at the surface close to the glass substrate. The ratio of sample thickness to the diffusion of carriers is much greater than 1, but it is much less than the dimensionless front surface recombination S_1. The pairs of free electrons and holes are photogenerated not only due to fundamental absorption of radiation but also due to photogeneration of electrons from the exponential tail of valence band to the exponential tail of conduction band, i.e., due to the Urbach photogeneration of carriers. The estimated values of semiconductor parameters: δ, E_0, A_1, A_2, E_1, E_3, $\alpha_{PC}(h\nu)$, $\alpha_{PEM}(h\nu, I_i)$, a_2, a_3, a_5, a_6,

$n(h\nu)$, $k(h\nu)$, $k_f(h\nu)$, $k_u(h\nu)$, $k_{ex}(h\nu)$, $\beta_{PC}(h\nu)$, $\beta_{PEM}(h\nu)$, $\beta_{ex}(h\nu)$, and $(\mu_e\tau_e+\mu_h\tau_h)$ versus I_i, were already reported in this paper. However, the spectral dependences of the estimated parameters must be taken very carefully in the range of higher photon energies. It is because the reported fitting of PC and PEM data was performed under the assumption that β_{PC} and β_{PEM} saturate, with the value 1, with increasing photon energies. This assumption is usually used in the PC and PEM investigations of semiconductors, but it does not seem to be good in the reported case of investigations on *a*-Si:H,F.

The change of sign of the PEM current with increasing illumination of the sample (see Fig. 4) suggest strong decrease of carrier diffusion length L and/or strong increase of total absorption coefficient k of radiation with increasing intensity. Of course, the first phenomenon exists because in the PC investigations the product of carrier lifetime and mobility was found to decrease by an increase of radiation intensity, i.e., by increase of concentration of excess carriers (see Fig. 12). However, the latter of the suggested phenomena seems to be very probable too. It can explain not only the change of sign of the PEM current but also the bad fitting of the PC data in the range of higher photon energies and the worsening influence of an increase of light intensity on the fitting (see Fig. 3). Obviously, in the case of fast recombination of carriers at the front semiconductor surface, the theory of PC predicts that the PC response passes through a maximum and then decreases with increasing absorption coefficient of radiation [see the general Eq. (22) as well as the simplified Eq. (25)]. When the absorption increases with the light intensity, the maximum value of PC must be shifted to smaller photon energies in the photon energy scale. Therefore, increasing radiation intensity, one can expect faster decrease of the theoretical curve with increasing photon energy, in the range of higher photon energies, and consequently better fitting of the experimental results with the theory (see Fig. 3). Something additional will occur when the increase of total absorption of radiation with increasing light intensity is evoked by the free-carrier absorption of the light. In this case, the quantum coefficients of electrons and holes photogeneration [see Eqs. (16) and (27)] must decrease with increasing intensity of radiation, i.e., with increasing concentration of excess carriers. This decrease becomes more important with increasing photon energy due to stronger absorption of the photons and due to larger photogeneration of carriers. So, the effective quantum coefficients β_{PC} and β_{PEM} should not attain the value unity for photons of high energy. It will also diminish the theoretically predicted PC and PEM responses in the high-photon-energy range and will improve the fitting of the experimental results. Additionally, for the intermediate photon energies, the increase of β_{PC} and β_{PEM} with increasing $h\nu$ will be much slower than that shown in Fig. 11. It can have an important influence on the shape of theoretically predicted spectral characteristics of PC and PEM responses because in this case the oscillatory changes of I_v with changing $h\nu$ (see Fig. 1) should be relatively more important for the change of magnitudes of the products $\beta_{PC}I_v$ and $\beta_{PEM}I_v$ to which the PC and PEM responses are proportional. Simultaneously, if the value of $K=wk$ is more comparative to the value of the phase shift Γ, the last terms in Eqs. (13) and (22), which are attributed to the interference effect, will no longer be negligible and they will appear in the transformed Eqs. (21) and (25). It will give an additional series of oscillations in the theoretically predicted spectral dependences of PC and PEM responses. Additional investigations on these subjects are in progress.

ACKNOWLEDGMENTS

The authors wish to thank the researchers of Centro di Studio per la Chimica dei Plasmi, Consiglio Nazionale delle Ricerche, Bari, Italy, for providing samples. One of the authors (M.N.) is indebted to the University of Bari for very kind hospitality and financial support which he obtained while staying in Bari twice in successive years. This work was partially supported by Ministero della Pubblica Istruzione (Italy), Centro Interuniversitario di Struttura della Materia (Italy), Gruppo Nazionale di Struttura della Materia (Italy), and Centraling Program Badoir Podstawowych) (Poland) under Contract No. CPBP-01-08-C-2.5.

APPENDIX

Using the phenomenological theory, the transport through a semiconductor, in presence of static electric field **E** and steady magnetic field **B**, under bulk photogeneration, is described by the following equations:

$$\mathbf{I}_e=e\mu_e n_e\mathbf{E}+eD_e\,\mathrm{grad}n_e-\mu_{He}\mathbf{I}_e\times\mathbf{B}\ , \tag{A1}$$

$$\mathbf{I}_h=e\mu_h n_h\mathbf{E}-eD_h\,\mathrm{grad}n_h+\mu_{Hh}\mathbf{I}_h\times\mathbf{B}\ , \tag{A2}$$

$$\frac{\partial n_e}{\partial t}=\beta_e kI-\frac{\Delta n_e}{\tau_e}+\frac{1}{e}\mathrm{div}\mathbf{I}_e\ , \tag{A3}$$

$$\frac{\partial n_h}{\partial t}=\beta_h kI-\frac{\Delta n_h}{\tau_h}-\frac{1}{e}\mathrm{div}\mathbf{I}_h\ , \tag{A4}$$

where $\mathbf{I}_e(I_{ex},I_{ey},I_{ez})$, $\mathbf{I}_h(I_{hx},I_{hy},I_{hz})$ represent the vectors of electron and hole current densities. The other parameters have the same meanings as in the text.

Using the conditions given in Sec. III B, the solution of Eqs. (A1)–(A4) results in the following differential equation for I_{ey}:

$$\frac{d^2I_{ey}}{dy^2}-\frac{I_{ey}}{L^2}=-e\beta_{PEM}k\frac{dI}{dy}\ , \tag{A5}$$

where L and β_{PEM} are given by Eqs. (14) and (15), respectively.

Considering the following boundary conditions:

$$I_{ey}=es_1\,\Delta n_e=es_{1h}\,\Delta n_h\quad(\text{for } y=0)\ , \tag{A6}$$

$$I_{ey}=-es_2\,\Delta n_e=-es_{2h}\,\Delta n_h\quad(\text{for } y=w)\ , \tag{A7}$$

and the appropriate distribution of light intensity in the semiconductor [Eq. (11)], Eq. (A5) can be relatively easily solved. When one knows the solution for I_{ey}, the short-

circuit PEM current which flows through the sample can be determined as

$$i_{\mathrm{PEM}}=(\mu_{He}+\mu_{Hh})Bl_z\int_0^w I_{ey}\,dy\ . \tag{A8}$$

Applying Eqs. (A3) and (A4) and the solution for I_{ey}, the PC current can be found from

$$i_{\mathrm{PC}}=el_zE_x\int_0^w(\mu_e\,\Delta n_e+\mu_h\,\Delta n_h)dy\ . \tag{A9}$$

[1]R. H. Bube, *Photoconductivity in Solids* (Wiley, New York, 1960).
[2]M. Nowak, Prog. Quantum Electron. **11**, 1 (1987).
[3]A. Amith, Phys. Rev. **116**, 793 (1959).
[4]D. C. Look, Phys. Rev. B **16**, 5460 (1977).
[5]A. R. Moore, Appl. Phys. Lett. **37**, 327 (1980).
[6]M. Nowak, Phys. Status Solidi A **80**, 691 (1983).
[7]M. Nowak, Zesz. Nauk. Politech. Slask. Ser. Mat.-Fiz. Gliwice **50**, 3 (1985).
[8]R. W. Wood, *Physical Optics* (MacMillan, New York, 1947), Chap. VI.
[9]G. Bruno, P. Capezzuto, G. Cicala, and F. Cramarossa, in *Proceedings of the 8th International Symposium on Plasma Chemistry, Tokyo, 1987,* edited by K. Akashi and A. Kimbara (Tokyo, 1987), Vol. 3, p. 1536.
[10]O. S. Heavens, *Optical Properties of Thin Solid Films* (Dover, New York, 1965).
[11]M. H. Brodsky and P. A. Leary, J. Non-Cryst. Solids **35&36**, 487 (1980).
[12]J. H. Schetzina, Phys. Rev. B **11**, 4994 (1975).
[13]F. Adduci, L. Baldassarre, G. Maggipinto, A. Minafra, and F. Levy, Phys. Status Solidi A **50**, 257 (1978).